Journal of Photochemistry and Photobiology A: Chemistry 203 (2009) 105–111

Contents lists available at ScienceDirect

Journal of Photochemistry and Photobiology A: Chemistry

journal homepage: www.elsevier.com/locate/jphotochem

Efficient photocleavage of DNA utilizing water soluble riboflavin/naphthaleneacetate substituted fullerene complex

Yunyan Gao[a], Zhize Ou[a,*], Guoqiang Yang[b], Lihua Liu[a], Mimi Jin[a], Xuesong Wang[c], Baowen Zhang[a,b,c], Lingxuan Wang[b]

[a] Department of Applied Chemistry, School of Science, Northwestern Polytechnical University, YouYi Xilu No. 127, Xi'an 710072, People's Republic of China
[b] CAS Key Laboratory of Photochemistry, Institute of Chemistry, Chinese Academy of Sciences, Beijing 100190, People's Republic of China
[c] Technical Institute of Physics and Chemistry, Chinese Academy of Sciences, Beijing 100190, People's Republic of China

ARTICLE INFO

Article history:
Received 9 August 2008
Received in revised form 9 December 2008
Accepted 29 December 2008
Available online 4 January 2009

Keywords:
Fullerene
DNA cleavage
Riboflavin
Supramolecular complex
Photoinduced electron transfer

ABSTRACT

Riboflavin (RF), a metabolizable endogenous pigment, can significantly enhance the water solubility of naphthaleneacetate modified fullerene C_{60} (NP-C_{60}) upon formation of a supramolecular complex (RF/NP-C_{60}). NP-C_{60} can quench the fluorescence of RF efficiently through static quenching mechanism. The resulting complex exhibits strong affinity to calf thymus DNA, as indicated by the hypochromism of its absorption spectra. Under anaerobic conditions, RF/NP-C_{60} complex displays much more efficient photocleavage of the DNA than RF itself due to the occurrence of electron transfer from DNA to NP-C_{60}.

1. Introduction

Fullerene derivatives are generally considered as powerful building blocks in material sciences and medical chemistry, owing to their unique photophysical and photochemical behaviors [1,2]. DNA photocleavage is one of the biological activities of fullerene derivatives, which is involved in the potential application of fullerene derivatives in biological systems and pharmaceutical fields [3–7]. Coupling of nucleic acid specific agents to fullerenes can lead to higher affinity of fullerene derivatives towards target DNA [8–10].

However, the well-known lack of solubility of fullerenes in water is a negative aspect for their applications. Among the various approaches to solve this problem, supramolecular method, such as mixing with water soluble polymers [11,12] or lipid membrane [13,14], inclusion into cyclodextrins [15–17] or calixarenes [18,19] to form host–guest complexes, construction of supramolecular assemblies with aromatic component through π–π stacking interactions [20,21], is of great interests.

Riboflavin (RF, vitamins B_2, Fig. 1), an important metabolizable endogenous photosensitizer, is widely distributed in human tissues in free and conjugated forms [22,23]. It participates in various biological reactions such as causing damage of DNA and other cell matrix components [24–26]. It also has been reported that flavin moiety can be attached to single-walled carbon nanotube (SWCNT) through π–π stacking interactions [27–29]. Recently, riboflavin has attracted attention because it can improve the solubility of SWCNT in water [30]. Inspired by these studies, we investigated the interaction between riboflavin and fullerene derivatives.

In the current work, NP-C_{60} is synthesized in which naphthaleneacetate group is introduced to fullerene core to increase the affinity of fullerene to DNA [31,32]. Riboflavin can interact with NP-C_{60} and construct a complex in water. RF/NP-C_{60} complex shows high affinity towards calf thymus DNA and could cause efficient photocleavage of DNA under anaerobic condition. These results indicate that riboflavin can act as a metabolizable solubilizer for fullerene derivatives and the RF/NP-C_{60} complex has potentials to be applied in the medical fields.

2. Experimental

2.1. Chemicals

Malonic acid, 4-dimethylaminopyridine (DMAP), 1-naphthaleneacetic acid, tetrahydrofuran (THF), N,N′-dicyclohexyl carbodiimide (DCC), diethylene glycol, n-tetrabutylammonium perchlorate were purchased from Acros Organics. Fullerene C_{60}, riboflavin, calf thymus DNA (CT DNA) and pBR322 plasmid DNA were purchased

* Corresponding author. Tel.: +86 29 88492914; fax: +86 29 88494174.
E-mail address: ouzhize@nwpu.edu.cn (Z. Ou).

1010-6030/$ – see front matter © 2009 Elsevier B.V. All rights reserved.
doi:10.1016/j.jphotochem.2008.12.026

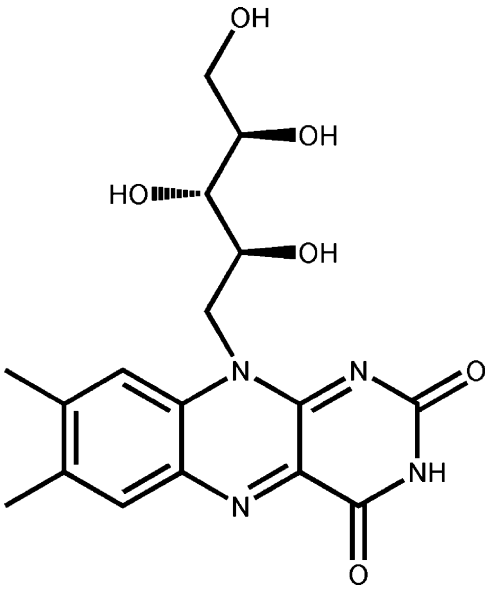

Fig. 1. Chemical structure of riboflavin (RF).

from Sigma Chemical Company. Other chemicals of analytical grade were obtained from Beijing Chemical Plant. The solvents were distilled before use. Water was freshly distilled twice before use.

All experiments involving DNA were performed in 10 mM Tris–HCl buffer (pH 7.4), unless otherwise noted. CT DNA solutions were prepared according to the literature [33]. The concentration of CT DNA was expressed as the concentration of nucleotide and calculated using an average molecular weight of 338 for a nucleotide and an extinction coefficient of 6600 M^{-1} cm^{-1} at 260 nm [34].

2.2. Synthesis

Compound ***1***. A solution of 1-naphthaleneacetic acid (1.5 g, 8.06 mmol) and DMAP (0.1 g, 0.82 mmol) and diethylene glycol (30 g, 283 mmol) in dry CH_2Cl_2 (120 mL) was cooled to −5 °C and stirred for 1 h. To this solution, DCC (2.6 g, 12.6 mmol) in 20 mL dry CH_2Cl_2 was added dropwise. After 10 h at −5 °C, the mixture was allowed to warm to room temperature. Water (200 mL) was added, and the resulting solution was extracted with $CHCl_3$ (3 mL × 50 mL). The combined organic extracts were washed with water solution of $NaHCO_3$. After solvent evaporation, the crude product was purified by flash chromatography (SiO_2, ethyl acetate/hexanes, 1/1) to yield **1** as colorless oil (1.5 g, 70% yield). ^{1}H NMR: (400 MHz, $CDCl_3$) δ 8.01 (d, J = 7.6 Hz, 1H), 7.99 (d, J = 7.6 Hz, 1H), 7.78–7.85 (m, 1H), 7.51–7.55 (m, 2H), 7.42–7.49 (m, 2H), 4.25 (m, 2H), 4.07 (s, 2H), 3.58–3.64 (m, 4H), 3.41 (t, J = 4.0 Hz, 2H), 1.63 (s, 1H). ^{13}C NMR (100 MHz, $CDCl_3$) δ 171.4, 133.6, 131.9, 130.2, 128.5, 127.9, 127.8, 126.2, 125.6, 125.3, 123.6, 72.2, 68.6, 63.8, 61.2, 38.8. MS (FAB^+), 296.7 [$(M+Na)^+$], calcd for $C_{16}H_{18}O_4Na$ 297.1.

Compound ***2***. To a solution of malonic acid (0.2 g, 1.9 mmol) and **1** (1.16 g, 4.2 mmol) in dry THF (40 mL) was added into a solution of DMAP (0.1 g, 0.82 mmol), DCC (0.87 g, 4.2 mmol) in dry THF (10 mL) dropwise over 30 min at room temperature. The reaction mixture was stirred for additional 20 h during which time a white precipitation was formed. The precipitation was filtered and washed with CH_2Cl_2 (3 mL × 20 mL), and combined organic fractions were evaporated. The crude product was purified with flash chromatography (SiO_2, ethyl acetate/hexanes, 2/1) to yield **2** as light yellow oil (1.2 g, 90%). ^{1}H NMR (400 MHz, $CDCl_3$): 7.98 (d, J = 8.0 Hz, 2H), 7.85 (d, J = 8.4 Hz, 2H), 7.78–7.80 (m, 2H), 7.47–7.51 (m, 4H), 7.40–7.51 (m, 4H), 4.23 (t, J = 4.7 Hz, 4H), 4.16 (t, J = 4.7 Hz, 4H), 4.09 (s, 4H), 3.60 (t, J = 4.8 Hz, 4H), 3.48 (t, J = 4.8 Hz, 4H), 3.39 (s, 2H). ^{13}C NMR (100 MHz, $CDCl_3$) δ 171.4, 166.3, 133.8, 132.1, 130.4, 128.7, 128.1, 128.0, 126.3, 125.8, 125.5, 123.8, 68.9, 68.7, 64.4, 64.0, 41.2, 39.0. MS (FAB^+), 639.6 [$(M+Na)^+$], calcd for $C_{35}H_{36}O_{10}Na$ 639.22.

Compound ***3*** (*NP-C_{60}*). C_{60} (50 mg, 0.069 mmol) and CBr_4 (34.8 mg, 0.106 mmol) were dissolved in anhydrous toluene (100 mL) with vigorous stirring. After degassing for 45 min, compound **2** (65.4 mg, 0.106 mmol) and DBU (20 μl, 0.16 mmol) were added and the mixture color changed gradually from purple to dark red. After stirring for 12 h, the solvent was removed under reduced pressure. The residue was purified with flash chromatography (SiO_2, toluene/ethyl acetate, 10/1) to yield **3** as brown solid (38.7%). ^{1}H NMR: (400 MHz, $CDCl_3$) 7.98 (d, J = 8.4 Hz, 2H), 7.77–7.84 (m, 4H), 7.41–7.53 (m, 8H), 4.48 (t, J = 4.5 Hz, 4H), 4.31 (t, J = 4.5 Hz, 4H), 4.10 (s, 4H), 3.61–3.63 (m, 8H). ^{13}C NMR: (100 MHz, $CDCl_3$) 171.39, 163.45, 145.28, 145.20, 145.18, 145.11, 144.92, 144.69, 144.64, 144.58, 143.89, 143.11, 143.03, 142.98, 142.20, 141.82, 140.94, 139.05, 133.83, 132.10, 130.44, 128.77, 128.13, 128.02, 126.40, 125.85, 125.52, 123.80, 71.39, 69.04, 68.60, 66.02, 64.08, 52.04, 39.08. MS (MALDI-TOF): m/z:1374.1 [$(M+K)^+$], calcd for $C_{95}H_{34}O_{10}K$ 1374.4. Elemental analysis, calcd for $C_{95}H_{34}O_{10}$: C, 85.45; H, 2.57. Found: C, 85.28; H, 2.64.

Preparation of RF/NP-C_{60} complex. Aqueous solution of NP-C_{60} was obtained according to the literature method [35], using RF as solubilizer. In detail, different amount of NP-C_{60} (0.1–2.7 mg) was added to 10 mL RF (0.2 mM) aqueous solution. The suspension was kept in a temperature-controlled (25 °C) sonicater (200 W) for 1.5 h, and then stirred at room temperature in the dark for 48 h. The insoluble NP-C_{60} was removed by centrifugation at 6000 rpm for 15 min. UV–vis spectrum was used to monitor whether NP-C_{60} was dissolved in water solution by examining the characteristic absorption maximum of precipitated NP-C_{60} in toluene. The obtained RF/NP-C_{60} solution was used for fluorescence and UV–vis spectra, and DNA cleavage experiment.

2.3. Measurements of spectral and electrochemical properties

The UV–vis absorption spectra and fluorescence emission spectra were recorded on a Hitachi U-3010 spectrophotometer and a Hitachi F-4500 fluorescence spectrometer, respectively.

Fluorescence lifetimes were measured by time-correlated single-photon counting technique with Edinburgh FL-900 spectrophotometer upon 400 nm laser pulse irradiation.

EPR spectra were obtained using a Bruker ESP-300E spectrometer operating at room temperature, and the operating conditions were as following: microwave bridge, X-band with 100 Hz field modulation; sweep width, 100 G; receiver gain, 1×10^5; microwave power, 5 mW. Samples were injected into the specially made quartz capillaries for analysis, purged with argon for 30 min in the dark, and illuminated directly in the cavity of the spectrometer with a Nd:YAG laser (355 nm, 5–6 ns pulse width, 10 mJ/pulse energy).

Cyclic voltammetry (CV) experiments were performed on a potentiostat/galvanostat Model 283A (EG&G Princeton Applied Research) in DMSO–toluene (9/1, v/v) solution, using two platinum wires as the working and counter electrodes, respectively, and a saturated calomel electrode (SCE) as reference electrode in the presence of 1 mM n-tetrabutylammonium perchlorate as the supporting electrolyte.

2.4. Melting temperature (T_m) determination of DNA samples

The absorption versus temperature was monitored at 260 nm using a U-3010 spectrometer with a temperature-controlled cell, and experiments were run in steps of 0.5 °C min^{-1} from 35 to 89 °C. The UV absorption curves were normalized from 0 (the absorbance at 260 nm of base line before the transition) to 1 (the absorbance at

260 nm at 89 °C) [36]. The midpoint of the inflection was taken as the corresponding melting temperature.

2.5. Examination of DNA-cleavage ability

An aqueous solution (10 μL) of pBR322 DNA (0.5 μg mL^{-1}) was diluted with 90 μL Tris–HCl buffer (10 mM, pH 7.4). An aqueous solution of riboflavin or RF/NP-C_{60} complex (30 μL), 30 μL of a buffer solution of pBR322 DNA (0.05 μg mL^{-1}), were mixed in a microtest tube to give the sample solution. The samples were purged with argon for 15 min in the dark to remove the air in the solution, and then incubated in dark or under irradiation for 10 min with high pressure mercury lamp and UV irradiation of λ < 300 nm is filtrated by Pyrex glass, and then mixed with 12 μL loading buffer, and loaded onto a 0.9% agrose gel containing ethidium bromide (10 μg mL^{-1}). The gels were run at a constant voltage of 90 V for 2 h in TAE (Tris–acetate–EDTA) buffer, washed with distilled water, visualized under a UV transilluminator, and photographed using an instant camera. The damage is defined as following equation (Eq. (1)) [37]:

$$\text{damage}\,(\%) = \frac{F_{\text{II}} - F_{\text{II0}}}{F_{\text{I0}}} \quad (1)$$

where the F_{II} and F_{II0} are the percentage of form II (nicked) of DNA with or without photosensitizer and F_{I0} is the percentage of form I of initial DNA.

3. Results and discussions

3.1. Absorption spectral studies

The general synthetic strategy toward NP-C_{60} is based on construction of malonate diethylene glycol ester terminated with naphthaleneacetate. The obtained malonate ester **2** was then coupled to C_{60}, following Bingel–Hirsch reaction, affording NP-C_{60} [38–40]. The synthetic route for the preparation of NP-C_{60} is outlined in Fig. 2.

Although soluble in toluene, chloroform and THF, NP-C_{60} is almost insoluble in more polar solvents, such as methanol, DMSO and water. In THF, NP-C_{60} exhibits three absorption peaks at 258, 326, and 426 nm, respectively (Fig. 3), typical of cyclopropanated fullerene [38]. In THF–H_2O (1/4, v/v) mixture, however, the absorption bands of NP-C_{60} shifts to longer wavelengths with peaks at 275 and 338 nm and the relative maximum at 426 nm is missing (Fig. 3), a sign of aggregate formation [41,42].

It has been reported that riboflavin can interact with SWCNT and enhance water solubility of SWCNT [30]. Here, we investigate the possibility that riboflavin might interact with NP-C_{60}. In the absence of riboflavin, NP-C_{60} is almost insoluble in water (<1 μM). While in the presence of riboflavin, the solubility of NP-C_{60} in polar solvents can be enhanced greatly. In detail, the concentration of NP-C_{60} in water can be up to 80 μM in aqueous riboflavin solution (0.2 mM).

The interaction between NP-C_{60} and riboflavin is further investigated by UV–vis absorption spectra. The UV–vis spectra of riboflavin in water show two peaks at 373 and 445 nm (Fig. 4a), respectively. Upon addition of NP-C_{60}, the absorption peaks increased gradually. Differential absorption spectra (Fig. 4b) display two peaks at 336 and 445 nm, respectively. The peak at 336 nm might be assigned to the absorption peak of NP-C_{60}, when compared with the absorption spectra of NP-C_{60} in THF–H_2O (9/1, v/v) (Fig. 4b inset). However, the peak at 445 nm cannot be ascribed to the absorption peak of NP-C_{60}, which may arise from the interaction of RF with NP-C_{60}.

The flavin adsorption energy onto SWCNTs is an order of magnitude higher in strength than that of an equicyclic anthracene [43]. A recent theoretical study indicated that the flavin moiety of flavin adenine dinucleotide (FAD) forms strong π–π interactions

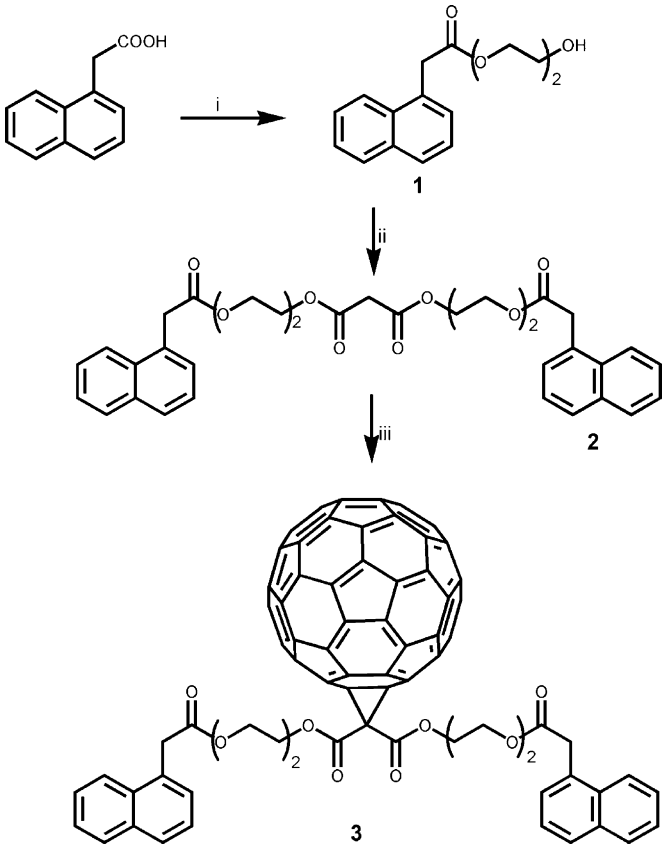

Fig. 2. Synthesis of compound **3** (NP-C_{60}). Reagents and conditions: (i) diethylene glycol, DCC, DMAP, CH_2Cl_2, −5 °C; (ii) malonic acid, DCC, DMAP, THF, rt; (iii) C_{60}, CBr_4, DBU, toluene, rt.

with SWCNTs, and the absorption spectra of RF would be changed after interaction with SWCNTs [27]. Taking insight into the structure of riboflavin, which possesses large aromatic rings, the nature of the interaction between riboflavin and NP-C_{60} may be attributed to π–π stacking interactions as in the case of non-covalent binding of aromatic components with C_{60} [44–47].

3.2. Fluorescence spectral studies

In DMSO–toluene solution, riboflavin shows a strong emission band at 512 nm with the excitation wavelength at 445 nm (Fig. 5a). The fluorescence intensity of riboflavin gradually decreases with the addition of NP-C_{60}. The dependence of the fluorescence intensity of riboflavin on the concentration of NP-C_{60} follows

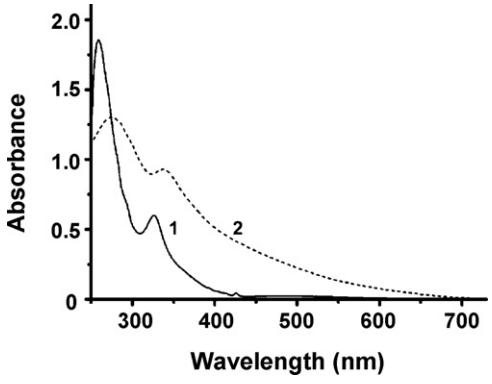

Fig. 3. Absorption spectra of NP-C_{60}. **1**, 20 μM in THF; **2**, 20 μM in THF–H_2O (1/4, v/v).

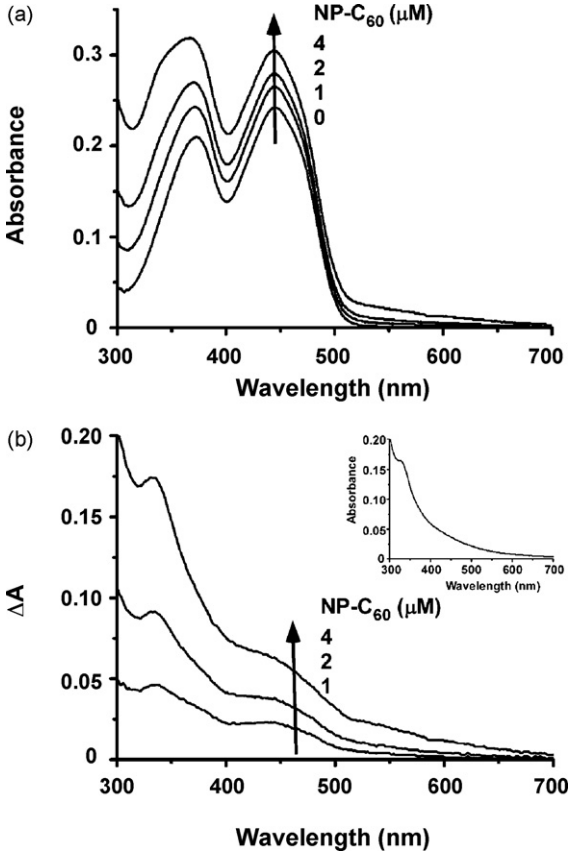

Fig. 4. (a) Absorption and (b) differential absorption spectra changes of riboflavin (20 μM) in H_2O upon addition of NP-C_{60} ($\Delta A = A_{RF/NP\text{-}C_{60}} - A_{RF}$). Inset: absorption spectrum of NP-C_{60} (4 μM) in THF–H_2O (1/9, v/v).

Stern–Volmer equation (Eq. (2)) [48], in which I_0 and I are the fluorescence intensity of riboflavin in the absence and in the presence of quencher (here NP-C_{60}), respectively. K_q is the quenching rate constant, τ_0 is the average fluorescence lifetime of riboflavin without quencher, and [Q] is the concentration of NP-C_{60}.

$$\frac{I_0}{I} = 1 + K_q \tau_0 [Q] \quad (2)$$

The fluorescence lifetime of riboflavin was measured to be 3.36 ns in toluene–DMSO solution by time-correlated single-photon counting technique. By fitting the fluorescence data to Stern–Volmer equation, the quenching rate constant (K_q) is estimated to be 8.6×10^{11} L mol^{-1} s^{-1} (the correlation coefficient is 0.9938). The apparent value of K_q is larger than that of the diffusion controlled limit (10^{10} L mol^{-1} s^{-1}), indicating some type of interaction between fluorophore and quencher [48]. To verify the possibility of dynamic quenching, fluorescence lifetime measurements are carried out. There is almost no change in lifetime of riboflavin after the addition of NP-C_{60} (3.28 ns). On the other hand, when increasing the temperature, the slope of the Stern–Volmer plot decreases (Fig. 5b). These results demonstrate that the fluorescence quenching mechanism is not dynamic but static. Effective quenching of the emission of riboflavin by NP-C_{60} is also observed in aqueous solution (Fig. 5c). A similar temperature-dependence of the Stern–Volmer plot suggests that NP-C_{60} quenches fluorescence of RF also through static quenching mechanism (Fig. 5d).

It has been reported that electron transfer can occur from excited riboflavin to strong electron acceptors, such as benzoquinone [49] and nitro blue tetrazolium [50]. Fullerene C_{60} is an excellent electron acceptor and can accept, reversibly, up to six electrons [51–53]. To investigate the possibility of electron-transfer reaction, it is important to determine the redox potentials of the relative reagents first. In DMSO–toluene (9/1, v/v), the oxidation potential of riboflavin is measured to be 2.58 V and the first reduction potential of NP-C_{60} to be −0.46 V (all potentials vs. SCE). The electron transfer from the excited state of riboflavin to the ground state of NP-C_{60} is a

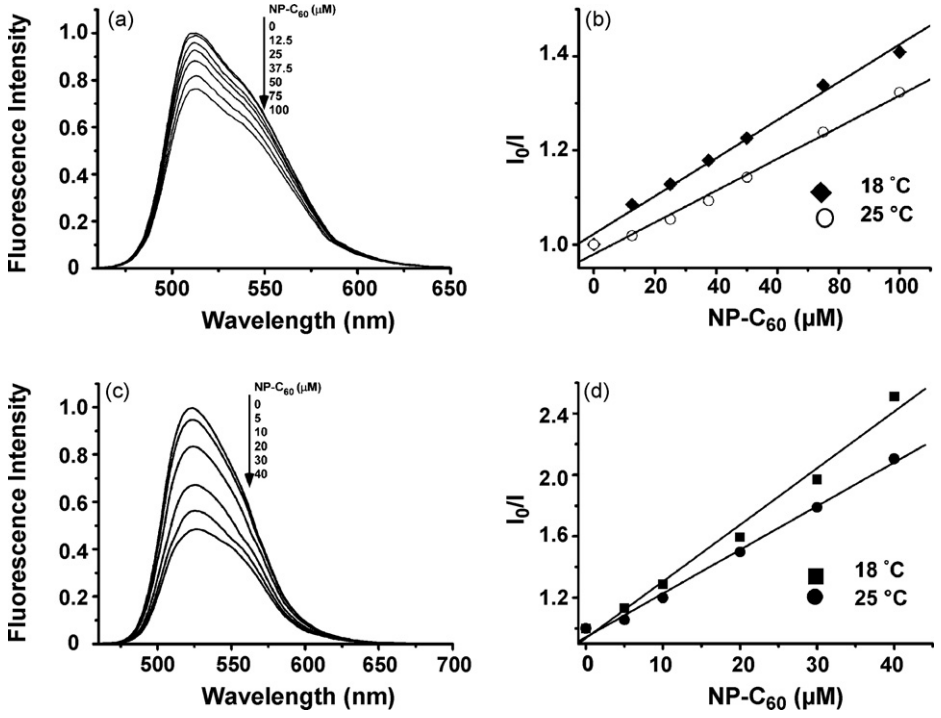

Fig. 5. (a) Fluorescence emission spectra changes (λ_{ex} = 445 nm) of riboflavin (100 μM) in DMSO–toluene (9/1, v/v) upon addition of NP-C_{60} at 25 °C. (b) Stern–Volmer plot for the fluorescence quenching of riboflavin at 512 nm by NP-C_{60} in DMSO–toluene (9/1, v/v). (c) Fluorescence emission spectra (λ_{ex} = 445 nm) of riboflavin (100 μM) upon addition of NP-C_{60} in H_2O at 25 °C. (d) Stern–Volmer plot for the fluorescence quenching of riboflavin at 524 nm by NP-C_{60} in H_2O.

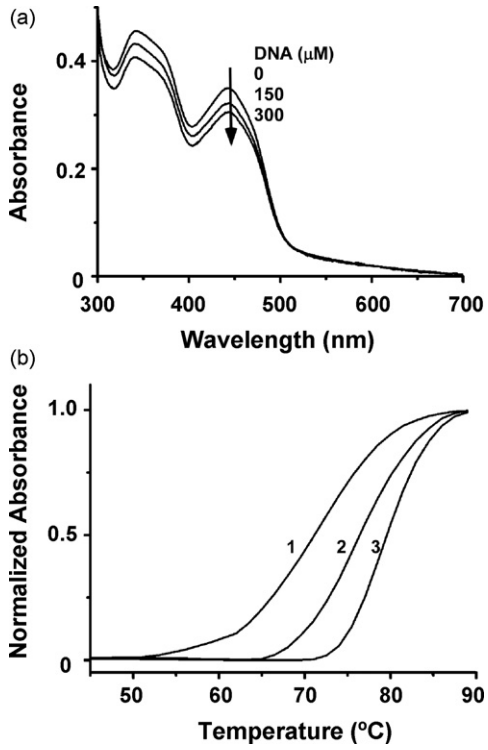

Fig. 6. (a) Absorption spectra of riboflavin (20 μM) and NP-C_{60} (8 μM) in the presence of different concentrations of CT DNA in buffer solution (pH 7.4). (b) Normalized melting curve of CT DNA (50 μM) with the addition of **1**, control; **2**, RF 10 μM; **3**, RF 10 μM, NP-C_{60} 4 μM.

thermodynamically unfavorable process ($\Delta G = 0.34$ eV), estimated by Rehm–Weller equation (Eq. (3)) [54], where the singlet excited state energy of riboflavin is 2.70 eV [55,56]:

$$\Delta G = E_{ox}(\text{donor}) - E_{red}(\text{acceptor}) - E_{0,0}(\text{excited state energy}) \quad (3)$$

As a result, the fluorescence quenching of riboflavin by NP-C_{60} is not *via* photoinduced electron transfer process, but due to the formation of nonfluorescent ground state complex between riboflavin and NP-C_{60}.

3.3. Affinity to CT DNA

Naphthalene derivatives [31,32] and riboflavin [57,58] possess ability to intercalate partially into the double helix DNA. Therefore, UV–vis absorption spectra and DNA melting temperature measurements are applied to investigate the interaction between CT DNA and RF/NP-C_{60} complex.

Fig. 6a shows the absorption spectra changes of RF/NP-C_{60} complex solution in Tris–HCl buffer upon titration of CT DNA. The addition of 300 μM CT DNA leads to an absorbance decrease at the absorption maximum (hypochromism) by 10.4% and 12.9% at the peaks of 338 and 445 nm, respectively. The free riboflavin undergoes similar absorption changes to a similar extent and hypochromism by 14.1% in the presence of 300 μM CT DNA at the peak of 445 nm. In contrast, due to the low solubility in water, free NP-C_{60} is only suspended in the DNA solution at the same concentration. Obviously, riboflavin enhances the solubility of NP-C_{60} and facilitates the interaction between CT DNA and NP-C_{60}.

It is expected that the interactions between a photosensitizer and CT DNA could also influence the properties of DNA itself to some extent. This is confirmed by DNA melting temperature measurements. Under our experimental condition, the melting temperature

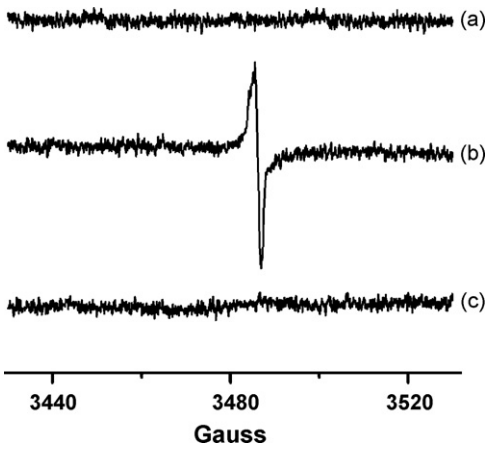

Fig. 7. (a) EPR spectra observed after laser pulse irradiation (355 nm) for 5 min in DMSO–buffer (1/1, v/v, pH 7.4) in the presence of RF (100 μM) and (a) NP-C_{60} (40 μM); (b) NP-C_{60} (40 μM), CT DNA (2 mM); (c) CT DNA (2 mM).

of CT DNA (50 μM) in buffer is measured to be 71.0 °C. When addition of riboflavin and RF/NP-C_{60} complex to the CT DNA solution, the melting temperature increases to 75.5 and 78.5 °C, respectively (Fig. 6b). A plausible explanation may be that both riboflavin and naphthalene group in NP-C_{60} can partially intercalate with CT DNA, making it more difficult for CT DNA to be detached to single strand and thus increasing the melting temperature of CT DNA.

3.4. Photosensitized damage on CT DNA

Photosensitizers bound to duplex DNA often react with nucleic acids through electron transfer to oxidize bases and the photoinduced electron transfer can cause efficient cleavage of DNA [59]. Upon irradiation of an argon-saturated DMSO–buffer solution of riboflavin and NP-C_{60}, no EPR signal can be observed (Fig. 7a). However, when DNA is introduced into the buffer solution of riboflavin and NP-C_{60}, a signal ($g = 2.000$) appears (Fig. 7b) after irradiation. The g value of the new signal agrees with that reported for $C_{60}^{-\bullet}$ [60–62], which suggests electron transfer from DNA to the excited state of NP-C_{60} occurs (Eq. (4)) [63]:

$$\text{DNA} + \text{NP-}C_{60}^{*} \rightarrow \text{DNA}^{+\bullet} + \text{NP-}C_{60}^{-\bullet} \quad (4)$$

Under our experimental conditions, when only riboflavin and DNA present in the buffer solution, no EPR signal is observed (Fig. 7c) after irradiation. Although it has been reported that electron transfer could occur from DNA to riboflavin [64], the EPR signal of riboflavin anion radical is usually observed under very low temperature (80 K) [64–66].

PBR322 plasmid DNA is employed as substrate to investigate the DNA-cutting ability of RF/NP-C_{60} complex under anaerobic condition. Control experiments show that DNA is not cleaved in the absence of photosensitizers or in the dark (Fig. 8, lanes 1–3). Under

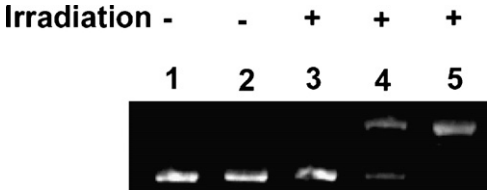

Fig. 8. Agrose gel electrophoretic patterns of pBR322 plasmid DNA. The reaction samples contained 0.3 μg of pBR322 plasmid DNA. Lanes 1 and 3: no reagent in 50 mM Tris–HCl (pH 7.4). Lanes 2 and 5: 10 μM RF, 4 μM NP-C_{60}. Lane 4: 10 μM RF. All samples are purged with argon for 15 min. Lanes 1 and 2 in the dark. Lanes 3–5, samples are irradiated with high pressure mercury lamp ($\lambda > 300$ nm) for 10 min.

irradiation, it can be seen that both riboflavin and RF/NP-C_{60} complex cause cleavage towards DNA (Fig. 8, lanes 4 and 5). Based on the percentage conversion from form I to form II for these photosensitizers, DNA-nicking efficiency was 49.8% for riboflavin and 74.5% for RF/NP-C_{60} complex, respectively. The increased photocleavage ability of RF/NP-C_{60}, compared with RF itself, is mainly from direct cleavage by NP-C_{60}. Due to the very low solubility of NP-C_{60} in water, DNA cleavage assay using NP-C_{60} itself is not carried out in this work.

Electron transfer from DNA to excited state C_{60} is one of the important DNA cleavage pathways by C_{60} derivative [63]. Fullerene C_{60}, an excellent three-dimensional electron acceptor, leads to remarkable acceleration of charge separation and deceleration of charge recombination [67,68]. As a result, RF/NP-C_{60} complex presents much stronger photocleavage ability on DNA than riboflavin under anaerobic conditions.

4. Conclusion

In summary, the endogenous pigment riboflavin can enhance water solubility of NP-C_{60} significantly and facilitate the interaction between NP-C_{60} and DNA. Under anaerobic condition, RF/NP-C_{60} complex displays much stronger photodamage ability on DNA than riboflavin, which can be attributed to the efficient electron transfer from DNA to NP-C_{60}.

Acknowledgments

This work supported by Youth Science and Technology Innovation Foundation of NPU (W016224), Ao Xiang Foundation for Youth NPU teachers (07XE0152), is gratefully acknowledged.

References

[1] E. Nakamura, H. Isobe, Functionalized fullerenes in water, Acc. Chem. Res. 36 (2003) 807–815.
[2] D.M. Guldi, G. Rahman, V. Sgobba, C. Ehli, Multifunctional molecular carbon materials—from fullerenes to carbon nanotubes, Chem. Soc. Rev. 35 (2006) 471–487.
[3] K. Kawai, Y. Wata, M. Hara, S. Tojo, T. Majima, Regulation of one-electron oxidation rate of guanine by base pairing with cytosine derivatives, J. Am. Chem. Soc. 124 (2002) 3586–3590.
[4] Y. Yamakoshi, N. Umezawa, A. Ryu, K. Arakane, N. Miyata, Y. Goda, T. Masumizu, T. Nagano, Active oxygen species generated from photoexcited fullerene (C_{60}) as potential medicines: $O_2^{-\bullet}$ versus $^1O_2$, J. Am. Chem. Soc. 125 (2003) 12803–12809.
[5] H. Tokuyama, S. Yamago, E. Nakamura, T. Shiraki, Y. Sugiura, Photoinduced biochemical activity of fullerene carboxylic acid, J. Am. Chem. Soc. 115 (1993) 7918–7919.
[6] J.L. Anderson, Y.Z. An, Y. Rubin, C.S. Foote, Photophysical characterization and singlet oxygen yield of a dihydrofullerene, J. Am. Chem. Soc. 116 (1994) 9763–9764.
[7] J.W. Arbogast, A.P. Darmanyan, C.S. Foote, Y. Rubin, F.N. Diederich, M.M. Alvarez, S.J. Anz, R.L. Whetten, The photophysical properties of C_{60}, J. Phys. Chem. 95 (1991) 11–12.
[8] M. Bergamin, T. Da Ros, G. Spalluto, A. Boutorine, M. Prato, Synthesis of a hybrid fullerene–trimethoxyindole–oligonucleotide conjugate, Chem. Commun. (2001) 17–18.
[9] Y.N. Yamakoshi, T. Yagami, S. Sueyoshi, N. Miyata, Acridine adduct of [60]fullerene with enhanced DNA-cleaving activity, J. Org. Chem. 61 (1996) 7236–7237.
[10] A. Boutorine, H. Tokuyama, M. Takasugi, H. Isobe, E. Nakamura, C. Helene, Singlet oxygen production from fullerene derivatives, Angew. Chem. Int. Ed. Engl. 33 (1994) 2462–2463.
[11] C. Ungurenasu, A. Airinei, Highly stable C_{60}/poly(vinylpyrrolidone) charge-transfer complexes afford new predictions for biological applications of underivatized fullerenes, J. Med. Chem. 43 (2000) 3186–3188.
[12] Y.N. Yamakoshi, T. Yagami, K. Fukuhara, S. Sueyoshi, N. Miyata, Solubilization of fullerenes into water with polyvinylpyrrolidone applicable to biological tests, J. Chem. Soc., Chem. Commun. (1994) 517–518.
[13] A. Ikeda, T. Sato, K. Kitamura, K. Nishiguchi, Y. Sasaki, J. Kikuchi, T. Ogawa, K. Yogo, T. Takeya, Efficient photocleavage of DNA utilising water-soluble lipid membrane-incorporated [60]fullerenes prepared using a [60]fullerene exchange method, Org. Biomol. Chem. 3 (2005) 2907–2909.
[14] A. Ikeda, Y. Doi, M. Hashizume, J. Kikuchi, T. Konishi, An extremely effective DNA photocleavage utilizing functionalized liposomes with a fullerene-enriched lipid bilayer, J. Am. Chem. Soc. 129 (2007) 4140–4141.
[15] C.N. Murthy, K.E. Geckeler, The water-soluble β-cyclodextrin–[60]fullerene complex, Chem. Commun. (2001) 1194–1195.
[16] K. Komatsu, K. Fujiwara, Y. Murata, T. Braun, Aqueous solubilization of crystalline fullerenes by supramolecular complexation with γ-cyclodextrin and sulfocalix[8]arene under mechanochemical high-speed vibration milling, J. Chem. Soc., Perkin Trans. 1 (1999) 2963–2966.
[17] Z. Yoshida, H. Takekuma, S. Takekuma, Y. Matsubara, Molecular recognition of C_{60} with γ-cyclodextrin, Angew. Chem. Int. Ed. Engl. 33 (1994) 1597–1598.
[18] A. Ikeda, T. Hatano, M. Kawaguchi, H. Suenaga, S. Shinkai, Water-soluble [60]fullerene–cationic homooxacalix[3]arene complex which is applicable to the photocleavage of DNA, Chem. Commun. (1999) 1403–1404.
[19] L. Atwood, G.A. Koutsantonis, C.L. Raston, Purification of C_{60} and C_{70} by selective complexation with calixarenes, Nature 368 (1994) 229–231.
[20] Y. Gao, Z. Ou, J. Chen, G. Yang, X. Wang, B. Zhang, M. Jin, L. Liu, Photodynamic properties of supramolecular assembly constructed by magnesium complex of hypocrellin A and fullerene C_{60}, New J. Chem. 32 (2008) 1555–1560.
[21] Y. Liu, H. Wang, Y. Chen, C. Ke, M. Liu, Supramolecular aggregates constructed from gold nanoparticles and L-try-CD polypseudorotaxanes as captors for fullerenes, J. Am. Chem. Soc. 127 (2005) 657–666.
[22] P.F. Heelis, The photophysical and photochemical properties of flavins (isoalloxazines), Chem. Soc. Rev. 11 (1982) 15–39.
[23] A. Bacher, H. Schnepple, B. Mailander, M.K. Otto, Y. Ben-Shaul, K. Yagi, T. Yamano, Flavins and Flavoproteins, Japan Scientific Society Press, Tokyo, 1980.
[24] C. Aubert, M.H. Vos, P. Mathis, A.P. Eker, K. Brettel, Intraprotein radical transfer during photoactivation of DNA photolyase, Nature 405 (2000) 586–590.
[25] A.M. Edwards, E. Silva, Effect of visible light on selected enzymes, vitamins and amino acids, J. Photochem. Photobiol. B: Biol. 63 (2001) 126–131.
[26] C.Y. Lu, S.D. Yao, N.Y. Lin, Photooxidation of 2′-deoxyguanosine 5′-monophosphate (dGMP) by flavin adenine dinucleotide (FAD) via electron transfer: a laser photolysis study, Chem. Phys. Lett. 330 (2000) 389–396.
[27] C.S. Lin, R.Q. Zhang, T.A. Niehaus, T. Frauenheim, Geometric and electronic structures of carbon nanotubes adsorbed with flavin adenine dinucleotide: a theoretical study, J. Phys. Chem. C 111 (2007) 4069–4073.
[28] S.Y. Ju, F. Papadimitrakopoulos, Synthesis and redox behavior of flavin mononucleotide-functionalized single-walled carbon nanotubes, J. Am. Chem. Soc. 130 (2008) 655–664.
[29] S.Y. Ju, J. Doll, I. Sharma, F. Papadimitrakopoulos, Selection of carbon nanotubes with specific chiralities using helical assemblies of flavin mononucleotide, Nature Nanotechnol. 3 (2008) 356–362.
[30] A. Casey, M. Davoren, E. Herzog, F.M. Lyng, H.J. Byrne, G. Chambers, Probing the interaction of single walled carbon nanotubes within cell culture medium as a precursor to toxicity testing, Carbon 45 (2007) 34–40.
[31] J.F. Hartwig, P.M. Pil, S.J. Lippard, Synthesis and DNA binding properties of a cisplatin analog containing a tethered dansyl group, J. Am. Chem. Soc. 114 (1992) 8292–8293.
[32] D.W. Dixon, N.B. Thornton, V. Steullet, T. Netzel, Effect of DNA scaffolding on intramolecular electron transfer quenching of a photoexcited ruthenium (II) polypyridine naphthalene diimide, Inorg. Chem. 38 (1999) 5526–5534.
[33] Z. Ou, J. Chen, X. Wang, B. Zhang, Y. Cao, Synthesis of a water-soluble cyclodextrin modified hypocrellin and ESR study of its photodynamic therapy properties, New J. Chem. 26 (2002) 1130–1136.
[34] H.J. Karlsson, M. Eriksson, E. Perzon, B. Akerman, P. Lincoln, G. Westman, Groove-binding unsymmetrical cyanine dyes for staining of DNA: syntheses and characterization of the DNA-binding, Nucleic Acids Res. 31 (2003) 6227–6234.
[35] C. Ehli, G.M.A. Rahman, N. Jux, D. Balbinot, D.M. Guldi, F. Paolucci, M. Marcaccio, D. Paolucci, M. Melle-Franco, F. Zerbetto, S. Campidelli, M. Prato, Interactions in single wall carbon nanotubes/pyrene/porphyrin nanohybrids, J. Am. Chem. Soc. 128 (2006) 11222–11231.
[36] Y. Zeng, A. Montrichok, G. Zocchi, Bubble nucleation and cooperativity in DNA melting, J. Mol. Biol. 339 (2004) 67–75.
[37] W. Zou, J. An, L. Jiang, Damage to pBR322 DNA photosensitized by hypocrellin A in liposomes and its derivative in solution, J. Photochem. Photobiol. B: Biol. 33 (1996) 73–78.
[38] X. Camps, A. Hirsch, Efficient cyclopropanation of C_{60} starting from malonates, J. Chem. Soc., Perkin Trans. 1 (1997) 1595–1596.
[39] C. Bingel, Cyclopropylation of fullerenes, Chem. Ber. 126 (1993) 1957–1960.
[40] A. Hirsch, I. Lamparth, V. Karfunkel, Fullerene chemistry in three dimensions: isolation of seven regioisomeric bisadducts and chiral trisadducts of c60 and di(ethoxycarbonyl)methylene, Angew. Chem. Int. Ed. Engl. 33 (1994) 437–438.
[41] S. Filippone, F. Heimann, A. Rassat, A highly water-soluble 2:1 β-cyclodextrin–fullerene conjugate, Chem. Commun. (2002) 1508–1509.
[42] V. Bensasson, E. Bienvenue, M. Dellinger, S. Leach, P. Seta, C_{60} in model biological systems: a visible–UV absorption study of solvent-dependent parameters and solute aggregation, J. Phys. Chem. 98 (1994) 3492–3500.
[43] J. Lu, S. Nagase, X. Zhang, D. Wang, M. Ni, Y. Maeda, T. Wakahara, T. Nakahodo, T. Tsuchiya, T. Akasaka, Z. Gao, D. Yu, H. Ye, W.N. Mei, Y. Zhou, Selective interaction of large or charge-transfer aromatic molecules with metallic single-wall carbon nanotubes: critical role of the molecular size and orientation, J. Am. Chem. Soc. 128 (2006) 5114–5118.
[44] E.M. Perez, M. Sierra, L. Sanchez, M.R. Torres, R. Viruela, P.M. Viruela, E. Orti, N. Martin, Fullerene complex with tetrathiafulvalene-type donors, Angew. Chem. Int. Ed. 46 (2007) 1847–1851.

[45] T. Kawase, N. Fujiwara, M. Tsutumi, M. Oda, Y. Maeda, T. Wakahara, T. Akasaka, Supramolecular dynamics of cyclic [6] paraphenyleneacetylene complexes with [60]- and [70]fullerene derivatives: electronic and structural effects on complexation, Angew. Chem. Int. Ed. 43 (2004) 5060–5062.
[46] M. Shirakawa, N. Fujita, S. Shinkai, Fullerene-motivated organogel formation in a porphyrin derivative bearing programmed hydrogen-bonding sites, J. Am. Chem. Soc. 125 (2003) 9902–9903.
[47] T. Hasobe, H. Imahori, P.V. Kamat, S. Fukuzumi, Quaternary self-organization of porphyrin and fullerene units by clusterization with gold nanoparticles on SnO_2 electrodes for organic solar cells, J. Am. Chem. Soc. 125 (2003) 14962–14963.
[48] J.R. Lakowicz, Principles of Fluorescence Spectroscopy, Plenum, New York, 1993.
[49] C.Y. Lu, Z.H. Han, G.S. Liu, X.C. Cai, Y.L. Chen, S.D. Yao, Photophysical and photochemical processes of riboflavin (vitamin B_2) by means of the transient absorption spectra in aqueous solution, Sci. China Ser. B: Chem. 44 (2001) 39–48.
[50] M. Takakubo, J. Faure, Riboflavin sensitized photoreduction of nitro blue tetrazolium ion (NBT^{2+}) in degassed aqueous solution, Photochem. Photobiol. 38 (1983) 137–140.
[51] N. Martin, L. Sanchez, B. Illescas, I. Perez, C_{60}-based electroactive organofullerenes, Chem. Rev. 98 (1998) 2527–2547.
[52] Q. Xie, E. Perez-Cordero, L. Echegoyen, Electrochemical detection of C_{60}^{6-} and C_{70}^{6-}: enhanced stability of fullerides in solution, J. Am. Chem. Soc. 114 (1992) 3978–3980.
[53] Y. Ohsawa, T. Saji, Electrochemical detection of C_{60}^{6-} at low temperature, J. Chem. Soc., Chem. Commun. (1992) 781–782.
[54] D. Rehm, A. Weller, Kinetics of fluorescence quenching by electron and H-atom transfer, Isr. J. Chem. 8 (1970) 259–272.
[55] A. Kathiravan, R. Renganathan, Photoinduced interaction between riboflavin and TiO_2 colloid, Spectrochim. Acta Part A 70 (2008), doi:10.1016/j.saa.2008.03.004.
[56] K. Kishore, P.N. Moorthy, S.N. Guha, Pulse radiolysis study of the one electron oxidation of riboflavin, Radiat. Phys. Chem. 38 (1991) 119–125.
[57] N.B. Sankaran, S. Nishizawa, T. Seino, K. Yoshimoto, N. Teramae, Abasic-site-containing oligodeoxynucleotides as aptamers for riboflavin, Angew. Chem. Int. Ed. 45 (2006) 1563–1568.
[58] K. Ito, S. Inoue, K. Yamamoto, S. Kawanishi, 8-Hydroxydeoxyguanosine formation at the 5′ site of 5′-GG-3′ sequences in double-stranded DNA by UV radiation with riboflavin, J. Biol. Chem. 268 (1993) 13221–13227.
[59] G.B. Schuster, Long-range charge transfer in DNA: transient structural distortions control the distance dependence, Acc. Chem. Res. 33 (2000) 253–260.
[60] A.L. Konkin, S. Sensfuss, H.K. Roth, G. Nazmutdinova, M. Schroedner, M. Al-Ibrahim, D.A.M. Egbe, LESR study on PPV–PPE/PCBM composites for organic photovoltaics, Synth. Met. 148 (2005) 199–204.
[61] M. Iyoda, S. Sasaki, F. Sultana, M. Yoshida, Y. Kuwatani, S. Nagase, Mono-and dianion of benzoquinone-linked [60] fullerene, Tetrahedron Lett. 37 (1996) 7987–7990.
[62] V. Brezova, A. Stasko, P. Rapta, G. Domschke, A. Bartl, L. Dunsch, Fullerene anion formation by electron transfer from amino donor to photoexcited C60: electron paramagnetic resonance study, J. Phys. Chem. 99 (1995) 16234–16241.
[63] R. Bernstein, F. Prat, C.S. Foote, On the mechanism of DNA cleavage by fullerenes investigated in model systems: electron transfer from guanosine and 8-oxoguanosine derivatives to C_{60}, J. Am. Chem. Soc. 121 (1999) 464–465.
[64] C. Pal, J. Huttermann, Postirradiation electron transfer vs. differential radical decay in X-irradiated DNA and its mixtures with additives: electron spin resonance spectroscopy in LiBr glass at low temperatures, J. Phys. Chem. B 110 (2006) 14976–14987.
[65] M. Hans, E. Bill, I. Cirpus, A.J. Pierik, M. Hetzel, D. Alber, W. Buckel, Adenosine triphosphate-induced electron transfer in 2-hydroxyglutaryl-CoA dehydratase from *Acidaminococcus fermentans*, Biochemistry 41 (2002) 5873–5882.
[66] R.M. Kowalczyk, E. Schleicher, R. Bittl, S. Weber, The photoinduced triplet of flavins and its protonation states, J. Am. Chem. Soc. 126 (2004) 11393–11399.
[67] D.M. Guldi, C. Luo, N.A. Kotov, T. Da Ros, S. Bosi, M. Prato, Zwitterionic acceptor moieties: small reorganization energy and unique stabilization of charge transfer products, J. Phys. Chem. B 107 (2003) 7293–7298.
[68] H. Imahori, K. Hagiwara, M. Aoki, T. Akiyama, S. Taniguchi, T. Okada, M. Shirakawa, Y. Sakata, Linkage and solvent dependence of photoinduced electron transfer in zincporphyrin-C_{60} dyads, J. Am. Soc. Chem. 118 (1996) 11771–11782.